Supplemental Information: Theory and optimisation of radiative recombination in broken-gap InAs/GaSb superlattices

Cónal Murphy,[1,2,a)] Eoin P. O'Reilly,[1,2] and Christopher A. Broderick[1,2,b)]
[1)]*Tyndall National Institute, University College Cork, Lee Maltings, Dyke Parade, Cork T12 R5CP, Ireland*
[2)]*School of Physics, University College Cork, Cork T12 YN60, Ireland*

(Dated: 4 September 2023)

I. COMPLEX BAND STRUCTURE

We work with an 8-band $\mathbf{k}\cdot\mathbf{p}$ Hamiltonian in the total angular momentum basis $|J;m_J\rangle$ of zone-centre Bloch states that diagonalise the spin-orbit interaction.[1,2] With $k_x = k_y = 0$ the Hamiltonian block diagonalises such that the heavy-hole (HH) valence band (VB) is decoupled, with the dispersion of the light-hole (LH) and spin-split-off (SO) VBs and the lowest energy conduction band (CB) along [001] then described by the 3×3 Hamiltonian

$$H_{3\times3}(k_z) = \begin{pmatrix} E_g + \frac{\hbar^2}{2m_0}s_c k_z^2 & \sqrt{\frac{2}{3}}Pk_z & -\frac{1}{\sqrt{3}}Pk_z \\ \sqrt{\frac{2}{3}}Pk_z & -\frac{\hbar^2}{2m_0}(\gamma_1+2\gamma_2)k_z^2 & \sqrt{2}\frac{\hbar^2}{m_0}\gamma_2 k_z^2 \\ -\frac{1}{\sqrt{3}}Pk_z & \sqrt{2}\frac{\hbar^2}{m_0}\gamma_2 k_z^2 & -\Delta_0 - \frac{\hbar^2}{2m_0}\gamma_1 k_z^2 \end{pmatrix} \begin{matrix} |\frac{1}{2};+\frac{1}{2}\rangle \\ |\frac{3}{2};+\frac{1}{2}\rangle \\ |\frac{1}{2};+\frac{1}{2}\rangle \end{matrix}, \tag{1}$$

where E_g is the band gap, Δ_0 is the VB spin-orbit splitting energy, and P is the inter-band (Kane) momentum matrix element, related to the Kane parameter via $E_P = \frac{2m_0P^2}{\hbar^2}$. The modified inverse CB edge effective mass s_c is given by

$$s_c = \frac{1}{m_c^*} - \frac{E_P}{3}\left(\frac{2}{E_g} + \frac{1}{E_g+\Delta_0}\right) \tag{2}$$

while the modified VB Luttinger parameters are defined as

$$\gamma_1 = \gamma_1^{\mathrm{L}} - \frac{E_P}{3E_g}, \tag{3}$$

$$\gamma_2 = \gamma_2^{\mathrm{L}} - \frac{E_P}{6E_g}, \tag{4}$$

where γ_1^{L} and γ_2^{L} are the bare VB Luttinger parameters.

We compute the complex band structure admitted by Eq. (1) using the eigenvalue method of Chang and Schulman.[3] We write Eq. (1) as $H_{3\times3}(k_z) = H^{(0)} + H^{(1)}k_z + H^{(2)}k_z^2$, where $H^{(0)}$, $H^{(1)}$ and $H^{(2)}$ are the 3×3 coefficient matrices for terms in Eq. (1) that are respectively independent of k_z, linear in k_z and quadratic in k_z. Using these coefficient matrices we construct the 6×6 "companion" matrix to $H_{3\times3}(k_z)$

$$C(E) = \begin{pmatrix} 0 & I \\ -(H^{(2)})^{-1}(H^{(0)}-EI) & -(H^{(2)})^{-1}H^{(1)} \end{pmatrix}, \tag{5}$$

where I is the 3×3 identity matrix.

Diagonalising Eq. (5) as a function of energy E then yields the, in general, complex-valued wave vectors $k_{z,n}(E, k_x = 0, k_y = 0)$. The parameters used in our complex band structure calculations are as described for the SL calculations in the main text.

II. SPURIOUS SOLUTIONS

Following the parameter renormalisation described in Sec. II C of the main text, we note that it is not possible to conclude that the impact of spurious solutions on the SL electronic structure calculated using the 8-band $\mathbf{k}\cdot\mathbf{p}$ Hamiltonian have been removed entirely. We will now demonstrate this explicitly. Firstly, we note that setting $s_c = 0$ allows for a discontinuity to occur at an InAs/GaSb interface in amplitude of the CB Bloch component of the envelope function.[4] Omitting the SO band by setting the VB spin-orbit splitting Δ_{SO} equal to zero allows us to reduce $H_{3\times3}$ of Eq. (1) to a 2-band Hamiltonian for the CB and LH states

$$H_{2\times2}(k_z) = \begin{pmatrix} E_c + ak_z^2 & Pk_z \\ Pk_z & E_v - bk_z^2 \end{pmatrix} \begin{matrix} |\frac{1}{2};+\frac{1}{2}\rangle \\ |\frac{3}{2};+\frac{1}{2}\rangle \end{matrix}, \tag{6}$$

where $a = \frac{\hbar^2 s_c}{2m_0}$ and $b = \frac{\hbar^2}{2m_0}(\gamma_1+4\gamma_2)$. We can use Eq. (6) to understand the origin of the aforementioned discontinuity in the envelope function, which gives rise to the step-like behaviour of the $e1$ probability density observed in Fig. 2(a) of the main paper. We do so by diagonalising Eq. (6) for small

[a)]Electronic mail: conalmurphy@umail.ucc.ie
[b)]Electronic mail: c.broderick@umail.ucc.ie

values of a (equivalent to small values of s_c) and then analyse the evolution of its eigenstates as $a \to 0$. Evaluating the determinant $|H_{2\times2} - E\,I| = 0$ produces a quartic characteristic equation in k_z, for which the solutions for small a are

$$k^2_{z,\pm}(E) \approx \frac{-\left(P^2 + b\,(E_c - E)\right) \pm \sqrt{\left(P^2 + b\,(E_c - E)\right)^2 - 4ab\,(E_c - E)\,(E - E_v)}}{2ab}. \tag{7}$$

In addition to the usual Kane solution $k^2_{z,+}$, which describes the evanescent band linking the VB and CB edges,[5] we also obtain a second solution $k^2_{z,-}$ whose value at small a can be approximated as

$$\kappa^2_-(E) \equiv -k^2_{z,-}(E) \approx \frac{P^2 + b\,(E_c - E)}{ab}, \tag{8}$$

with $\kappa^2_- \to \infty$ as $a \to 0$. The corresponding eigenstates of $H_{2\times2}$ approach $|\psi_+\rangle = e^{\pm\kappa_+ z}|\frac{1}{2};+\frac{1}{2}\rangle$ as $a \to 0$, where $|\frac{1}{2};+\frac{1}{2}\rangle$ is the $k_z = 0$ CB Bloch (basis) state.[2] To calculate allowed energy states in a heterostructure grown along the z direction, we replace $k_z \to -i\frac{\mathrm{d}}{\mathrm{d}z}$ in Eq. (6).[6] Writing this quantised Hamiltonian as

$$\widehat{H}\psi = A\,\frac{\mathrm{d}^2\psi}{\mathrm{d}z^2} + B\,\frac{\mathrm{d}\psi}{dz} + C\psi, \tag{9}$$

then the allowed solutions must satisfy the boundary conditions that both ψ and $A\,\frac{\mathrm{d}\psi}{\mathrm{d}z} + \frac{1}{2}B\psi$ are continuous,[6] where

$$A = \begin{pmatrix} -a & 0 \\ 0 & b \end{pmatrix},\ B = \begin{pmatrix} 0 & iP \\ -iP & 0 \end{pmatrix},\ \text{and } C = \begin{pmatrix} E_c & 0 \\ 0 & E_v \end{pmatrix}, \tag{10}$$

are the respective coefficient matrices of Eq. (6) for terms that are quadratic in k_z, linear in k_z, and independent of k_z.

These boundary conditions appear to mandate that the CB component of ψ must always be continuous. However, the term $A\,\frac{\mathrm{d}\psi}{\mathrm{d}z}$ can allow for a jump discontinuity in the amplitude of ψ as $a \to 0$. For $E \approx E_c$ we have $\frac{\mathrm{d}\psi_-}{\mathrm{d}z} \approx \pm\frac{P}{\sqrt{ab}}\psi_-$, so that the CB component of $A\,\frac{\mathrm{d}\psi}{\mathrm{d}z}$ can then vary as $-a\,\frac{\mathrm{d}\psi_-}{\mathrm{d}z} \approx \mp P\sqrt{\frac{a}{b}}\,\psi_-$, which vanishes as $a \to 0$. This behaviour, discussed by Foreman in the $a = 0$ limit,[4] accounts for the observed discontinuities in the $e1$ envelope function at InAs/GaSb interfaces in the full 8-band calculations (cf. Fig. 2(a), main text).

We note that our calculated InAs and GaSb bulk complex band structures, using renormalised parameters with $s_c = 0$ (cf. Fig. 1(b), main text), are in good quantitative agreement with the results of atomistic tight-binding calculations over the same ranges of energy and wave vector.[7] States from outside of these ranges of energy and wave vector also contribute, albeit less strongly, to the determination of the variation of the electron envelope function with position in a full atomistic calculation. However, as described in the main text, our renormalised 8-band $\mathbf{k}\cdot\mathbf{p}$ calculations capture the key features of the envelope functions and inter-band optical matrix elements observed in the full atomistic SL calculations of Refs. 8 and 9. This demonstrates that the impact of spurious solutions is sufficiently mitigated to validate our $\mathbf{k}\cdot\mathbf{p}$ calculations of the InAs/GaSb SL electronic structure as a platform to predict and analyse trends in radiative recombination.

III. ENVELOPE FUNCTION EVOLUTION ALONG MINIBANDS

In the main text we noted that the optical (momentum) matrix element between the $\mathbf{k}_\parallel = 0$ $e1$ and $h1$ SL eigenstates goes to zero as q is varied from zero to $\frac{\pi}{L}$ (cf. Fig. 3(a), main text). This behaviour was attributed to the introduction of a relative phase shift between the $e1$ and $h1$ envelope functions as the minibands are traversed in q. To illustrate this explicitly, we present here the calculated Bloch components of the $e1$ and $h1$ envelope functions at both $q = 0$ and $\frac{\pi}{L}$. We recall that since the HH band is decoupled at $\mathbf{k}_\parallel = 0$, the $e1$ eigenstate consists of an admixture of CB, LH and SO Bloch character only, while the $h1$ eigenstate is purely HH-like.

The results of these calculations are summarised in Fig. 1, which shows the aforementioned non-zero envelope function Bloch components at $q = 0$ (top row) and $q = \frac{\pi}{L}$ (bottom row) for a single SL period. Panels (a), (b) and (c) in the top row, and (e), (f) and (g) in the bottom row, respectively show the CB, LH and SO components of the $e1$ eigenstate. Panels (d) and (h) show the HH component of the $h1$ eigenstate at $q = 0$ and $\frac{\pi}{L}$, respectively.

Considering first the Bloch components of the $e1$ eigenstate, at $q = 0$ the CB (LH and SO) component is purely real and even (imaginary and odd) about the centre of the InAs layer (shaded region) at $z = 0$, and remains so as q changes from zero to $\frac{\pi}{L}$. For the $h1$ state, we observe changing phase and parity between $q = 0$ and $\frac{\pi}{L}$, with the HH Bloch component changing from being purely real and even about the centre of the InAs layer at $q = 0$ to purely real and odd about the centre of the InAs layer at $q = \frac{\pi}{L}$. This directly demonstrates that varying q from zero to $\frac{\pi}{L}$ introduces a difference in parity between the $e1$ and $h1$ SL eigenstates at $\mathbf{k}_\parallel = 0$. This results in the $e1$ and $h1$ eigenstates having equal (opposite) parity at $q = 0$ ($q = \frac{\pi}{L}$) which, combined with the respective s- and p-like symmetry of the CB and HH Bloch basis states $|\frac{1}{2};\pm\frac{1}{2}\rangle$ and $|\frac{3}{2};\pm\frac{3}{2}\rangle$, gives rise to the calculated reduction of the $\mathbf{k}_\parallel = 0$ $e1$-$h1$ inter-band optical matrix element to zero at the SL Brillouin zone edge (cf. Fig. 3(a), main text).

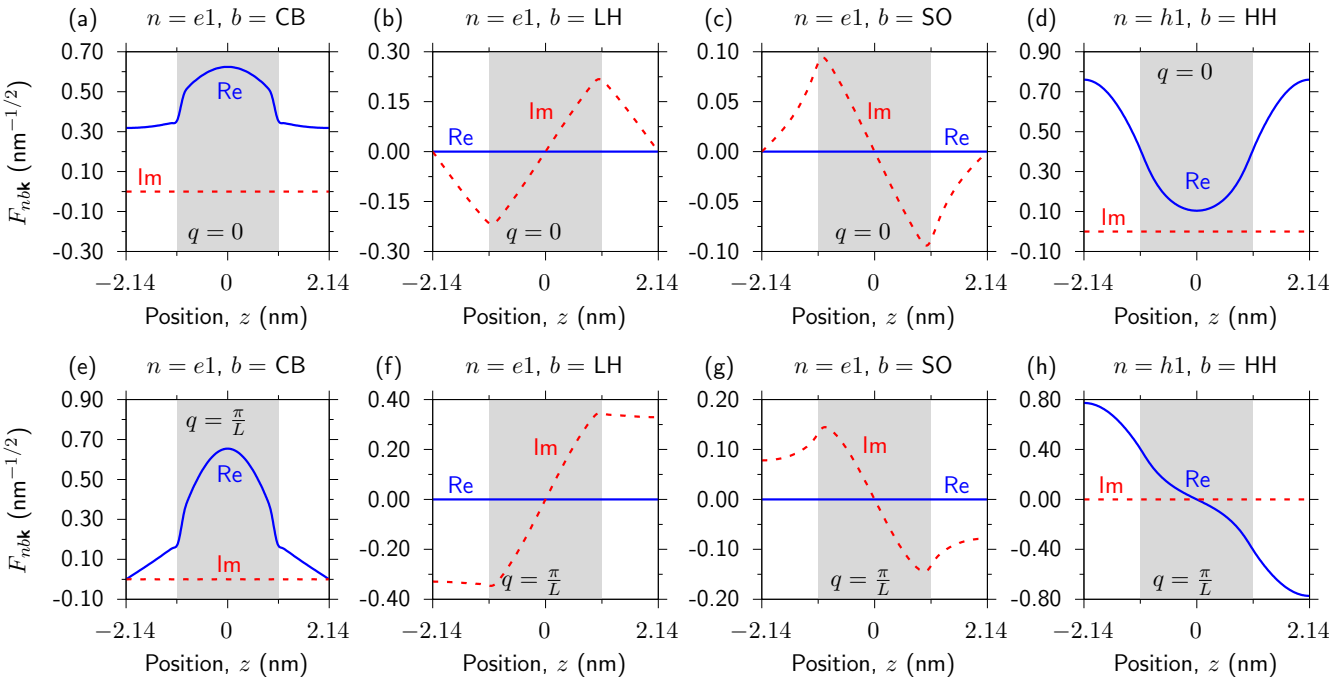

FIG. 1. Top row: real (solid blue lines) and imaginary (dashed red lines) parts of the $q = 0$ envelope function Bloch components $F_{nb\mathbf{k}}(z)$ for the $\mathbf{k}_\parallel = 0$ $e1$ and $h1$ eigenstates of the exemplar equal layer thickness InAs/GaSb SL considered in the main text (having SL period $L = 2t = 4.28$ nm). (a) CB component of $e1$, (b) LH component of $e1$, (c) SO component of $e1$, and (d) HH component of $h1$. Bottom row: as in the top row, but for $q = \frac{\pi}{L}$. Shaded (unshaded) regions denote the electron-confining InAs (hole-confining GaSb) layers.

We note that the fact that this change in parity is restricted to the $h1$ eigenstate in Fig. 1 is a consequence of the specific choice of calculational supercell. Here, we have utilised a supercell $z \in [-\frac{L}{2}, \frac{L}{2}]$ which is centred about the centre of the electron-confining InAs layer. Changing to, for example, a supercell with $z = 0$ set at the centre of the hole-confining GaSb layer instead produces a change in the phase and parity of the $e1$ eigenstate as q varies from zero to $\frac{\pi}{L}$, with the parity of the $h1$ eigenstate then remaining fixed. This emphasises that it is the *difference* in parity between the $e1$ and $h1$ eigenstates that determines their inter-band optical matrix element, irrespective of a given choice of calculational supercell.

[1]A. B. Cohen and G. E. Marques, "Electronic structure of zinc-blende-structure semiconductor heterostructures," Phys. Rev. B **41**, 10608 (1990).

[2]T. B. Bahder, "Eight-band **k**·**p** model of strained zinc-blende crystals," Phys. Rev. B **41**, 11992 (1990).

[3]Y. C. Chang and J. N. Schulman, "Complex band structures of crystalline solids: an eigenvalue method," Phys. Rev. B **25**, 3975 (1982).

[4]B. A. Foreman, "Elimination of spurious solutions from eight-band **k**·**p** theory," Phys. Rev. B **56**, R12748 (1997).

[5]S. Das, C. A. Broderick, and E. P. O'Reilly, "Impact of band-anticrossing on band-to-band tunneling in highly-mismatched semiconductor alloys," Phys. Rev. Applied **17**, 014029 (2022).

[6]B. Chen, M. Lazzouni, and L. R. Ram-Mohan, "Diagonal representation for the transfer-matrix method for obtaining electronic energy levels in layered semiconductor heterostructures," Phys. Rev. B **45**, 1204 (1992).

[7]J. N. Schulman and Y. C. Chang, "Band mixing in semiconductor superlattices," Phys. Rev. B **31**, 2056 (1985).

[8]T. Kato and S. Souma, "sp^3s^* tight-binding calculation of band edges and effective masses of InAs/GaSb superlattices with different interface structures," Superlatt. Microstruct. **122**, 492 (2018).

[9]Y. C. Chang and J. N. Schulman, "Interband optical transitions in GaAs-$Ga_{1-x}Al_xAs$ and InAs-GaSb superlattices," Phys. Rev. B **31**, 2069 (1985).